CORE
Metadata, citation and similar papers at core.ac.uk
Provided by UCL Discovery

Fuel 108 (2013) 356–369

Contents lists available at SciVerse ScienceDirect

Fuel

journal homepage: www.elsevier.com/locate/fuel

Thermodynamic modelling and evaluation of a two-stage thermal process for waste gasification

Massimiliano Materazzi [a,b], Paola Lettieri [a,*], Luca Mazzei [a], Richard Taylor [b], Chris Chapman [b,*]

[a] Department of Chemical Engineering, University College London, Torrington Place, London WC1E 7JE, UK
[b] Advanced Plasma Power, South Marston Business Park, Swindon SN3 4DE, UK

HIGHLIGHTS

- This paper compares single and multiple stages gasification technologies.
- A model is developed to predict efficiency and gas composition at each stage.
- The model is validated with experimental data taken from a demonstration plant.
- Carbon conversion and syngas yield are enhanced when using a two-stage process.
- Optimal oxidants ratio and energy demand depend on the aims of different projects.

ARTICLE INFO

Article history:
Received 15 August 2012
Received in revised form 17 September 2012
Accepted 14 February 2013
Available online 6 March 2013

Keywords:
Gasification
Waste
Equilibrium model
Fluidized bed
Plasma

ABSTRACT

Tar generation and ash disposal represent the strongest barrier for use of fluid bed gasification for waste treatment, whereas sufficing for both is only possible with expensive cleaning systems and further processing. The use of plasma within an advanced two-stage thermal process is able to achieve efficient cracking of the complex organics to the primary syngas constituents whilst limiting the electric power demand. This study focused on the thermodynamic assets of using a two-stage thermal process over the conventional single-stage approach. These include, for example, the fact that the primary thermal waste decomposition is performed in conditions of optimal stoichiometric ratio for the gasification reactants. Furthermore, staging the oxidant injection in two separate intakes significantly improves the efficiency of the system, reducing the plasma power consumption. A flexible model capable of providing reliable quantitative predictions of product yield and composition after the two-stage process has been developed. The method has a systematic structure that embraces atom conservation principles and equilibrium calculation routines, considering all the conversion stages that lead from the initial waste feed to final products. The model was also validated with experimental data from a demonstration plant. The study effectively demonstrated that the two-stage gasification system significantly improves the gas yield of the system and the carbon conversion efficiency, which are crucial in other single stage systems, whilst maintaining high energy performances.

© 2013 Elsevier Ltd. All rights reserved.

1. Introduction

Energy generation and waste disposal are two of the most difficult challenges facing the world today. As the world's fossil fuel resources are depleted, we are facing a mounting crisis of energy supply. At the same time, global population growth and rising living standards increase the energy demand, and the resulting amount of waste material produced is dramatically higher than ever before. Waste-to-Energy (WtE) technologies have an important role to play in resetting this balance. In this context, there is considerable interest in new ways to dispose of waste using thermal conversion technologies, particularly gasification and pyrolysis. Waste gasification, latest addition to Waste-to-Energy technologies, converts solid wastes into green electricity or clean gaseous fuel known as synthesis gas (or syngas). This promising technology has received increasing attention in the past two decades due to the growing demand for clean fuels and chemical feedstocks, as well as the need for reducing dependency on fossil fuels, lowering green house gas emissions and disposing of existing wastes. In general all the advanced thermal conversion technologies, which include gasification and pyrolysis, are increasingly being preferred to incineration and combustion in waste to energy

* Corresponding authors. Tel.: +44 207 6707867; fax: +44 207 3832348 (P. Lettieri), tel.: +44 (0)1793 238523; fax: +44 1793 828 287 (C. Chapman).
E-mail addresses: p.lettieri@ucl.ac.uk (P. Lettieri), chris.chapman@app-uk.com (C. Chapman).

0016-2361/$ - see front matter © 2013 Elsevier Ltd. All rights reserved.
http://dx.doi.org/10.1016/j.fuel.2013.02.037

Nomenclature

n_i	molar flowrate of gaseous species *i*, kmol/h
b_j	total number of atoms of the *j*th element
a_{ij}	number of atoms of the *j*th element present in a molecule of chemical species *i*
f_i	fugacity of species *i*, bar
P	pressure, bar
R	universal gas constant, 8.314 kJ/kmol K
T	temperature, K
P_i	partial pressure of species *i*, bar
ϕ	fugacity coefficient
y_i	mole fraction of gas species *i*
$\Delta\overline{G}^0_{f,i}$	standard Gibbs free energy of formation of species *i*, kJ/kmol
$\Delta\overline{H}^0_{f,i}$	standard enthalpy of formation of species *i*, kJ/kmol
$\Delta\overline{S}^0_{f,i}$	standard entropy of formation of species *i*, kJ/kmol K
G^{tot}	total Gibbs free energy of the system, kJ/h
$\overline{C}_P$	heat capacity at constant pressure, kJ/kmol K
ΔH	net enthalpy rate, kJ/h
Q_{loss}	heat loss, kJ/h
W_{power}	electric power from plasma, kJ/h
$\sum H$	total stream enthalpy rate, kJ/h
$\dot{m}$	mass flowrate, kg/h

Abbreviations

WtE	waste to energy
FBG	fluidized bed gasifier
PCBs	polychlorinated biphenyls
RDF	refuse derived fuel
PAHs	polycyclic aromatic hydrocarbons
IGCC	integrated gasification combined cycle
SR	stoichiometric ratio
MSW	municipal solid waste
TOC	total organic carbon
SOFC	solid oxide fuel cell
GHV	gross heating value, MJ/kg
LHV	lower heating value, kJ/kmol

Superscripts

$'$	stage one
$''$	stage two
$^\circ$	standard reference state

Subscripts

r	reactant
p	product
i	*i*th gas species
j, *k*	*j*th, *k*th chemical element
IN	flux in
OUT	flux out
comp	component
(*g*)	gas phase
(*s*)	solid phase
(*v*)	vapour phase

Greek letters

ν_i	stoichiometric coefficient of species *i*
α,β	char conversion splitting factors
μ_i	chemical potential of species *i*, kJ/kmol
GRG	generalized reduced gradient
FTIR	Fourier transform infrared spectroscopy
VBA	visual basic for applications
ASR	automotive shredder residue
C&I	commercial and industrial
VOC	volatile organic carbon
CGE	cold gas efficiency
OPR	oxygen partition ratio
NEE	net electrical efficiency
SNG	synthetic natural gas

applications. The advantages include higher recycling rates, lower emissions, higher energy efficiencies, lower costs, smaller footprints and reduced visual impact [1].

Most of the gasification systems from waste are based on high-temperature techniques that use oxygen as a source of heat or as partial oxidation agent. On this regard, there are numerous advanced oxygen-blown gasifiers that are at various stages of development [2–4]. Among all waste gasification technologies, fluidized bed reactors are the most promising, for a number of reasons [5]. In particular, the enhanced flow mixing between reactants, the nearly constant temperature and the great operating flexibility of fluidized bed reactors make it possible to utilize different types of feedstock, including biomass and solid wastes. These gasifiers usually work as "partial combustors", and a portion of the carbon present in the fuel is combusted to support pyrolysis and gasification reactions. Because of the relatively low temperature used to prevent agglomeration and sintering of bed material, the gas that is produced by a standard fluid bed gasifier (FBG) has tars and other condensable organic species that are technically difficult and costly to remove. Furthermore, the bottom ash/char that is generated in the gasifier or pyrolysis fluid bed reactor may contain high levels of carbon, heavy metals and organic pollutants which lower the conversion efficiency of the process and limit any secondary usage. The ash/char residue can be up to 20% of the weight of the incoming material and must be further processed before being landfilled [6]. Tar generation and ash disposal represent the strongest barrier for use of FBG for waste treatment, whereas sufficing for both is only possible with expensive cleaning systems and further processing.

The use of plasma systems has increasingly been applied with thermal waste treatment for its ability to completely decompose the input waste material into a tar-free synthetic gas and an inert, environmentally stable, vitreous material known as slag. The principal advantages that plasma offers to thermal conversion processes, besides the already mentioned tar/ash related issues absence, are a smaller installation size for a given waste throughput, and the use of electricity as energy source, characteristics which permit the technology to treat a wide range of low calorific value materials including liquids and solids. Because of these potential advantages, plasma technologies have been developed for the destruction and removal of various hazardous waste, such as PCBs [7], medical waste [8], metallurgical wastes, incineration fly ash [9], and low-level radioactive wastes. Its efficient application in the treatment of general waste is still under debate though, due to the power required to convert the solid waste to a gas. Only additions of combustion heat supplied by the waste feedstock or a fuel additive make the process suited to large waste streams. Examples of technology development include InEnTec in USA and Alter NRG, in Japan [10].

In applying the plasma technology to the gaseous products from a thermal gasifier, an advanced two-stage thermal process is able to achieve efficient cracking of the complex organics to the primary syngas constituents whilst limiting the electrical energy demand of the process. Forerunners in this approach are Advanced Plasma

Power (APP) in the UK and Plasco Energy Group Inc., Canada [11]. The technical innovation of this approach is to initiate pyrolysis using a conventional gasifier and use plasma power to refine the gas by decomposing and converting the tars, tailoring the syngas for efficient electricity production in gas engines and vitrifying the hot solid residue. The result is large net electricity production while still maintaining excellent environmental standards.

This study focuses on an advanced two stage fluid bed gasification – plasma converter technology approximately reproducing the Gasplasma® process licensed by the UK company APP [12]. The feedstock consists of different types of refuse derived fuel (RDF) produced from a combination of residual municipal, commercial and industrial wastes. The aim of this study is to develop a flexible model for two-stage processes, capable of providing reliable quantitative predictions of product yield and composition. The model has a systematic structure that embraces atom conservation principles and equilibrium calculation routines, considering all the conversion stages that lead from the initial waste feed to final products. In this manner, a tool able to predict the final composition of the gas, given specified proximate and ultimate analysis of the feed and process operating conditions (pressure, mass flowrate of waste stream, oxidants/feed ratio), is obtained. The same approach can also be used for a parametric study optimizing the effect of the operating parameters (flowrate of gasification agents, plasma power input) on the producer gas composition, its heating value and the process efficiency. The analysis is systematically supported by experimental data from a demonstration plant.

2. Gasification concepts

The physical and chemical processes which take place between the gasification agents and the fresh solid feed in the conversion route to synthesis gas are complex, influenced by varying feed, process design and operating conditions; nonetheless, the gasification chemistry may be considered as a two distinct conversion mechanisms. When biomass particles are rapidly heated at high temperature (above 600 °C) in the reactor, more than 80% of their (dry) mass is rapidly converted into permanent gases and organic vapours, leaving only a variable amount of char and few mineral ashes in the solid phase. With high volatility (more than 60%) and low ignition temperature (250–350 °C), RDF starts to devolatize immediately after the injection of the fuel into the reactor [13]. This first step is usually referred to as pyrolysis, wherein water vapour, organic liquids and non-condensable gases, such as CO, H_2, CO_2, are separated from the solid carbon (i.e. char) and ash content of the fuel. The vapour/liquid product comprises mostly of polyaromatic hydrocarbons (PAHs) and tar (i.e. dark, oily, viscous material, consisting mainly of heavy organic and mixed oxygenates). Subsequently, the volatiles and char undergo a second gasification step and they modify their composition due to the occurrence of several reactions becoming the final syngas (see Table 1). Most of these reactions are endothermic and require a consistent amount of energy to proceed.

The distinction between primary and secondary conversion is based on the different times of conversion of the various processes. Experimental studies have shown that as a result of the rapid heating of the fuel, 90% of devolatilization takes place in a matter of milliseconds, whereas the reminder of gasification processes (mainly heterogeneous reactions) take one or two orders of magnitude longer time [14]. In this sense, char gasification is the most important and critical of all reactions. Though char from biomass usually constitutes a minor fraction of the fuel, its conversion kinetics has a major effect on the performance of a gasifier, for it is the slowest of conversion processes.

From this general concept originates the idea of dividing the gasification process in two different reactor design arrangements, namely ‘single-stage’ and ‘multi-stage’ groups.

2.1. Single stage process

The aim of a ‘single-stage’ gasifier is to convert organic substances entirely in one reactor. Depending on the type of operation, the solid fuel is injected into a hot environment, together with oxygen and steam.

As the fuel particles devolatize, the hydrocarbons volatiles undergo gas-phase reaction with the most reactive species in the ambient gas, that is, oxygen. Thus, the oxygen supplies the required heat by reacting with the reactive volatiles [15]. The most commonly used gasification technologies for ‘single-stage’ processes are fixed bed (up-draft, down-draft, side-draft), entrained bed and fluidized bed reactors (bubbling bed, circulating fluidized bed, spout fluid bed) [16]. A brief comparison of the types of gasification technologies that are utilized for single-stage solid waste gasification is provided in Table 2.

Fixed bed gasifiers use a bed of solid fuel particles through which oxidants and gas pass either up or down. They are the simplest type of gasifiers and generally operate with high carbon conversion, long solid residence time, low gas velocity and low ash carry over. Fixed beds in single stage mode are usually limited to high grade fuels gasification either by bed stability, or by incipient fluidization and overheating issues. This technology is being considered to be of average strength only for small-scale heat and power applications [17]. Entrained-flow gasifiers are all oxygen blown, slagging gasifiers producing medium heating value syngas [18]. This technology has many advantages such as high efficiency and throughput, and relatively low content of higher hydrocarbons or tars in syngas. For this reason, it is one of the widest used technologies for large power generation applications in IGCC plants and chemical synthesis. However, even after several decades of commercialization on coal treatment, the availability of entrained flow gasifiers is still limited for waste treatment applications. The

Table 1
Typical gasification reactions [5].

Reaction name	Biomass gasification	Energy (kJ/mol)
Exothermic		
Combustion	$(Char/Volatiles)C + O_2 \rightarrow CO_2$	−398.3
Partial oxidation	$(Char/Volatiles)C + 1/2O_2 \rightarrow CO$	−123.1
Water gas shift	$CO + H_2O \leftrightarrow H_2 + CO_2$	−40.9
CO methanation (I)	$CO + 3H_2 \leftrightarrow CH_4 + H_2O$	−217.0
CO methanation (II)	$2CO + 2H_2 \leftrightarrow CH_4 + CO_2$	−257.0
Endothermic		
Pyrolysis	$Biomass \rightarrow Char + Volatiles + CH_4 + CO + H_2 + N_2$	+200–400
Methane steam reforming	$CH_4 + H_2O \leftrightarrow CO + 3H_2$	206.0
Water gas/steam carbon	$(Char/Volatiles)C + H_2O \rightarrow CO_2 + H_2$	118.4
Boudouard	$(Char/Volatiles)C + CO_2 \rightarrow 2CO$	159.9

Table 2
Comparison of single-stage gasification technologies [11,32].

	Fixed bed	Fluidized bed	Entrained flow	Plasma
Key feed characteristics	Mixed plastic wastes	Mixed plastic wastes, shredded MSW, sludges, metal rich wastes	Mixed plastic wastes. Not suited to untreated MSW	MSW (+tyres, ASR), RDF, petcoke, hazardous wastes
	Particle diameter up to 100 mm	Particle diameter up to 100 mm	Particle diameter smaller than 1 mm, water is added to produce the slurry	No size requirements
Temperature (°C)	Large temperature gradients: from 500° (pyrolysis zone) to 1200° (combustion zone)	Temperature is almost constant, in the range of 700 – 1000°	The range is 1200–1500°, above the ash melting temperature	Usually very high, typically between 1500° and 5500°
Pressure (bar)	1–100	1–30	20–80	1–30
Residence time	Particles stay in the bed until their discharge Normally 900–1800 s at high pressure	Particles spend long time (minutes or hours) in the bed Gas residence time depends on gas velocity, normally 10–100 s	Very short (1–5 s)	Defined by the specific process. Few seconds for the gas phase, minutes or hours for the solid
Heat exchange	Inefficient exchange. Necessity of large surface of heat exchanger	Very efficient heat transfer	Poor exchange (dominated by radiation)	Exchange dominated by radiation
Conversion	High conversion is possible with adequate temperature control	High conversion is possible with adequate flow mixing	Conversion can be high	Conversion can be as high as 100%
Bottom ash quality	Low leaching bottom ash. TOC[a] <3%	Low leaching bottom ash. TOC[a] 0.5–1%	Low leaching slag	Vitrified, inert, no leaching slag

[a] TOC: total organic carbon.

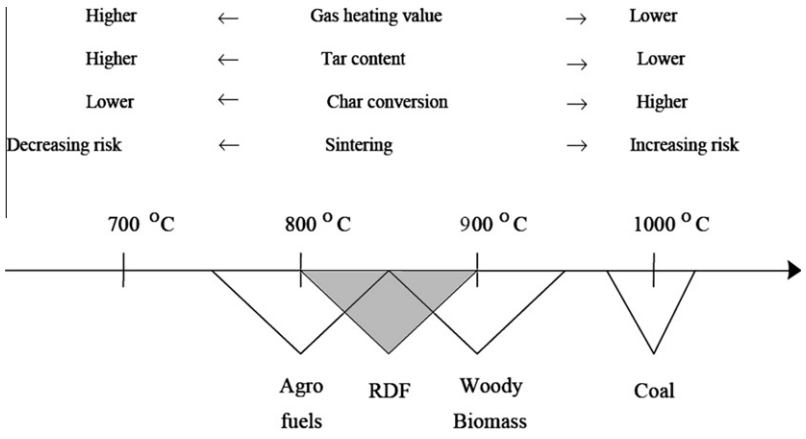

Fig. 1. Typical gasification temperature for various feedstock and influence of temperature change on some critical factors as reported by Hallgren [21,22].

gasifier's short residence time (seconds) requires the feedstock to be pulverized to less than 1 mm, which make this technology very unsuitable for general waste processing [19]. Fluid bed systems allow a more efficient gasification due to a homogeneous temperature, good flow mixing inside the reactor, rapid heating of the biomass feedstock, and the possibility of including catalyst in the bed inventory to enhance the reforming reactions. They are suitable for various types of feedstock and can be scaled up to relatively large plant sizes. The conversion of char and tar in these reactors relies on a number of physical conditions including temperature, heating rate, residence time and degree of dispersion of the particles in the bed. The fate of the volatiles produced depends, in addition, on the background gas composition, that is, if the pyrolysis is carried out in steam, the product would be mainly carbon monoxide and hydrogen [20].

Fig. 1 is a composite that illustrates the effect of temperature in FBG on some key output variables: char conversion, tar concentration, heating value of producer gas, and ash sintering risk. As we could expect, raising the temperature to certain levels generally enhances the kinetics of slow reactions, producing higher yields of synthesis gas. However, working at high temperatures increases the melting danger of various mineral phases in the system, and promotes coalescence of solid particles. Alkali-induced agglomeration and defluidization of the bed may cause severe operational problems and can be detrimental to the overall process. Furthermore, a higher temperature not always corresponds to a cleaner syngas; many authors have reported that even at the highest temperature acceptable, it is challenging to convert all the PAHs into syngas by non-catalytic reactions or by contact with bed material [19]. This is mainly due to the effect of the additional oxygen added to sustain such high temperatures, which also represent a key factor for the process performance. In fact, the temperature in the gasifier is usually controlled by the oxidant flow which sustains the exothermic oxidation reactions. At the same time, oxygen represents the main reactant for the chemical conversion of biomass/char particles. Its quantity relatively to fuel addition may conventionally be represented by the stoichiometric ratio (SR), which is the oxygen/fuel ratio divided by that corresponding to complete combustion.

Fig. 2 illustrates the effect of change with increasing oxidant addition as the system moves from gasification to combustion. The chemical energy in the gas increases with SR up to a certain le-

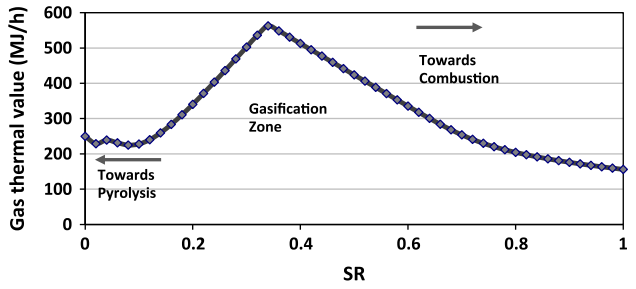

Fig. 2. Influence of SR on gas thermal value from gasification of RDF (30 kg/h of dry MSW).

vel because more volatiles are emitted and more char is converted with increasing temperature. This usually occurs from a stoichiometric ratio of 0.1 up to 0.3–0.4, depending on the composition of the RDF. However, when the minimum oxygen to carbon ratio is exceeded, more fuel is burned to CO_2 and H_2O and the heat release increases at the cost of product gas, lowering the chemical energy in the gas. This effect is more evident when high quantities of moisture and ash are present in the feedstock material and the oxidant supply rate must be enhanced to generate sufficient heat to sustain the gasification reaction. This represents one of the major drawbacks of working with autothermal gasifiers.

Staging of the gasification agent is a valid improvement to create different thermal levels in the gasifier, optimizing the total oxidant input. However, experimental studies [23] showed that injection of secondary oxygen at constant SR, i.e. analyzing the effect of injection in an isolated way, is effective for reduction of phenols and other light tar compounds, but the total tar concentration is still high (a few grams per Nm^3) and the proportion of stable aromatic tar compounds in the gas increases significantly. Only the use of an external source of heat would disconnect the chemical oxygen demand for a specific application from the thermal level required to sustain the gasification reactions. Electrically driven ionized gases, such as plasmas, have been involved in fuel conversion and combustion systems over a century and were originally used as a convenient thermal energy source to initiate combustion reactions. Only recently, plasmas have been investigated for their potential to exhibit catalytic effects primarily because of complex interactions of their excited species (electrons, ions, radicals) in fuel conversion reactions [24,25]. The independent source of heat of the gasifier is a plasma arc, which allows control of temperature independently from fluctuations in the feed, attaining a nearly constant syngas quality [26]. The Joule heating effect is responsible for high gas temperatures in thermal plasmas where power is initially transferred from the electric field to electrons and then to the background neutral gas species by way of a large number of electron-neutral collisions [27]. As a result, any organic molecules in the vicinity break down due to the high temperature conditions and the presence of highly reactive atomic and ionic species, forming a virtually clean synthetic gas [26]. Furthermore, fusion occurs for all inorganic components (glass, metals, silicates, heavy metals) into inert and stable vitrified slag, which finds several applications in construction industry [28].

In the one stage mode, pyrolysis or gasification is sustained by applying thermal plasma directly onto the waste material, with all of the energy required for decomposition coming from the plasma. This usually corresponds to a low overall energy efficiency because the high energy cost to create the plasma is often comparable to, if not greater than, the heating value of the obtained product [29]. Single-stage plasma gasification processes consume approximately 800 kW h electricity per ton of MSW, corresponding to approximately 2000 kW h of primary energy (assuming an average efficiency of 40% for electricity generation) which is close to the total energy contained in one ton of MSW (i.e. 2500 kW h) [11]. For this reason thermal arc plasma gasification is more used in the treatment of medical and hazardous waste, where a safe and environmentally friendly waste disposal with no harmful emissions is more important than energy production. On the other hand, the syngas produced by single-stage FBG can be used only if the requirements placed on product gas quality are low, as is the case for direct thermal gas use such as co-combustion of hot raw gas in coal boilers [30] or use as fuel gas in a cement process [31].

2.2. Two stage process

The basic concept of a two-stage design is to physically separate the principal unit operations of pyrolysis-preliminary gasification zone from the final conversion zone, involving two different levels of heat intakes. A few similar processes have been proposed for incineration processes based on two staged conversion; examples are Europlasma in France [33] and Ebara in Japan [34]. Applications in waste gasification are more attractive from an energetic point of view, for their unquestionable advantages in producing gas that can be used directly in a power generation process. Most of this type of advanced thermal processes eliminates char gasification as a limiting process step and, consequently, the efficiency of the process depends on how the conversion is organized. In a single stage process, the residual char reacts heterogeneously with the steam and CO_2 with a slow and highly endothermic process that is often accelerated to practical rates by the use of additional oxygen to keep the temperature high. The concept of two-stage gasification is based on providing longer residence time whilst making a more efficient use of the oxygen required to support the endothermic steam reactions. This results in higher yield of synthesis gas than is possible by single stage partial oxidation [16]. Most such processes have been based on two sequential reactors where this can be achieved more easily. Furthermore, the separation and control of the unit operations provides the means for the independent optimization of each operation.

Ebara Co. and Ube Industries Ltd. (Japan) developed a pressurized waste gasification process consisting of the direct combination of a fluid bed gasifier and a high temperature furnace used to generate synthesis gas from plastic packaging waste [35]. Wastes are first gasified in a medium temperature fluid bed to convert most of the fuel into syngas, and the ash is continuously discharged from the bottom of the bed. The second stage is a cyclonic furnace which utilizes the heating value of the gas to decompose dioxins and convert the ash to a molten slag. A first plant of this technology is located in Ube City (Japan) and has a capacity of 30 *t*/*d* of plastic packaging waste [35].

Advanced Plasma Power (UK) developed a two stage process (the Gasplasma process) which combines fluid bed gasification with plasma technology (Fig. 3). The fact that the final stage of the thermal process uses plasma as energy source instead of the energy content of the syngas makes the system more suitable for low-energy fuels, such as household and industrial wastes that often cannot sustain their own gasification without additional fuel.

The following description is focused on the core components of the two-stage thermal process developed at APP: the fluidized bed gasifier and the plasma converter.

The gasifier is a bubbling fluidized bed operated in temperature range between 650° and 800 °C, with the actual operating conditions depending on fuel characteristics and desired reaction profiles. The gasifier contains a bed of sand particles, and is fluidized with a supply of steam and oxygen whose flow is controlled to maintain the bed temperature and the required degree of fluidization. The gasifier's main function is to decompose the waste and to separate the combustibles and small ash particles from larger inert

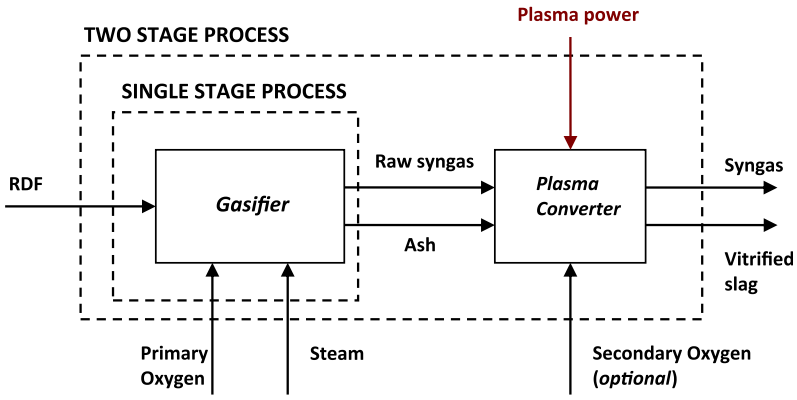

Fig. 3. Schematic of the Gasplasma two-stage thermal process.

and metallic particles. The organic components of the RDF (i.e., carbon and hydrogen based material, including food waste, yard waste, paper, plastic, rubber, textiles, etc.) are converted into a fuel gas, which flows upward in the reactor. The fuel gas is in a "raw" state, containing combustion gases ($H_2O + CO_2$), tar, fine char, fly ash, and hydrocarbons, in addition to carbon monoxide (CO) and hydrogen (H_2) typically found in a gasification synthesis gas. The percentage of these components in the fuel gas depends on the broader range of feedstock types and C/O ratio used. At the same time, dense inorganic materials (i.e., glass, metals, bones, and stones) drop by gravity to the bottom of the reactor. These materials are removed from the bottom of the reactor, along with some of the sand medium that is used as the fluidized bed of the gasifier. Sand is recycled back to the gasifier and the solid residues, including tramp material, are recovered for recycling or fed to the plasma converter for further treatment.

Fuel gas and carbonaceous particles, both produced in the gasifier, are upgraded together in the second stage of the process: a single carbon electrode plasma furnace at temperatures between 1100–1200 °C. Unlike some other gasification technologies, there is no need of intermediate fuel gas cleanup between the gasifier and the ash melting plasma converter. An addition of secondary oxygen feed assists in the breakdown of long chain hydrocarbons and ensures full conversion of carbonaceous residuals to a syngas virtually free of condensable liquids and tars. The gas flow pattern is intended to produce a slow cyclonic action to promote the separation of particulates from the syngas and also to maximize the residence time in the converter. The fine ash particles are collected on the walls, where they are vitrified and proceed slowly down through the furnace. The solid residues extracted from the gasifier and screened from the sand are also fed to the plasma converter and vitrify into a molten slag. This molten (i.e., vitrified) slag flows slowly down the furnace walls and is continuously discharged at the bottom of the furnace. As the slag is discharged, it is immediately cooled in a water bath. This quenching process results in the slag being pulverized into a glassy, granulate material, which is marketed as a construction material. The plasma power is controlled, along with the secondary oxygen inlet, to provide a uniform syngas temperature and destruction of the residual tars and chars contained within the crude syngas. An inert gas is also supplied to the plasma furnace as plasma gas and is usually introduced through a hole down the centre of the electrode.

Downstream of the plasma converter, the syngas can be directed straight to a SOFC stack for power generation, or cooled to around 200 °C in a steam boiler prior to cleaning treatment to remove any residual particulates and acid gas contaminants. The refined gas can be then used for power generation (gas engines or gas turbines), for conversion to a liquid fuel, or used as a chemical precursor.

3. Gasification model

3.1. Equilibrium model

The design and operation of a gasification process requires understanding of the influence of fuel and operating parameters on the performance of the plant. Especially for a two stage process, modelling results can provide guidance on the optimization of the gasification parameters, so that one can find the best operation condition between the two stages. Numerous models for gasifiers have been developed [36–42]. Recent gasification modelling efforts combined an equilibrium model with several kinetic constraints for particular reactor types to reproduce the performance of commercial gasifiers [36,42].

Equilibrium models, which take into account only thermodynamic limitations, thereby disregarding specific reaction mechanisms and transport rate phenomena, have long been applied to the prediction of product compositions in relation to changes in the operating conditions, providing an invaluable tool for process design and development purposes [41]. A literature analysis has shown that, generally, equilibrium models fail in matching experimental results when the reactor temperature is below 800 °C [40,41]; particularly, these models are unsuccessful for methane and hydrogen estimated content in the gas [42]. On the contrary, these models give good correlation at elevated temperatures (above 1000 °C) that occur on advanced thermal processes, yielding predictions in close accord with experimental observation.

A further assumption that is not always valid for practical gasifiers is that the residence time is sufficiently long to reach the equilibrium state [43]. Although determining the intrinsic kinetics of all the reactions may be difficult, a multiple stage route sensibly enhances the residence time of the gas. Initially, the conversion of char and tar, whose kinetic represents the rate limiting step of the process, is related to the effective time of exposure with the hot gas, which in turn depends on the local conditions in the first stage. In a bubbling fluidized bed, flow mixing is generally highly favoured; the interplay of mixing–segregation phenomena relevant to volatile matter release and conversion in fluidized bed was comprehensively studied by researchers at the University of Naples [44], who provided direct evidence of "endogenous" bubble formation and fuel particle segregation. The released volatiles form endogenous bubbles around the devolatilizing particles, lifting coarse fuel particles to the bed surface. Fuel particles remain segregated at the bed surface as far devolatilization is active, whereas the residual char is continuously re-circulated in the bed once devolatilization is complete. Thus, entrainment of coarse char particles during the first stage is negligible in a bubbling unit, whereas entrainment of finer char particles may be severe [45]. The second

stage plays a critical role in this sense; the furnace geometry is intended to produce a slow cyclonic action to avoid short circuiting of particles, which receive maximum exposure to the intense ultra violet light within the converter. Kinetic restrictions are then avoided by the synergy between high operating temperature and long residence time in the process, so the system closely approaches equilibrium.

3.2. Thermodynamic equilibrium formulation

At this level of analysis, the gasification is treated from a purely thermodynamic point of view, and therefore the results are applicable to both stages, namely, single stage gasifier and plasma converter. For a given set of inlet conditions (feed composition and oxidant flowrates), the exit conditions are computed assuming thermodynamic equilibrium.

Two basic approaches can be used for chemical equilibrium calculations: algebraic and differential. The former is conceptually the easier of the two to understand and it is based on the simultaneous calculation of equilibrium constants for a given set of constituent reactions. An example of this method is the series reactor model, where a certain number of independent reactions proceed to equilibrium sequentially, and the process is repeated iteratively until the extent of reaction in each reactor is below some tolerance. The second approach, also known as non-stoichiometric approach, minimizes the total Gibbs free energy (G) of the system subject to the mass balance of individual elements and non-negativity constraints. The method that best fits the case in point for solving the simultaneous chemical equilibrium problem is the G-minimization technique, for it does not require knowledge of any independent set of chemical reactions, whose characterization turns out to be quite difficult in this process. The Gibbs method is based on the concept that at chemical equilibrium the total Gibbs energy of the system has its minimum value. By attempting to minimize the total energy of the system, individual equilibria constants are not considered. Rather, the possible reaction species are noted, and the distribution of these species is established using a general mathematical technique to give a minimum free energy for the system. The solution so achieved will satisfy all expected equilibria and be accurate within the limits of the thermodynamic data. The equilibrium formulation here presented follows the general framework of single-stage equilibrium models long reported in the literature [38,39].

As listed in Table 3, 43 species are considered in the system, including a variety of hydrocarbons, oxygenates and PAHs; this is quite easily accomplished with this method as there is no need to specify the reaction network. The ash is considered to be inert, adding only to the thermal capacity in the reactor.

For a system at constant temperature and pressure, the criterion of equilibrium is given by:

$$dG = \sum_{i=1}^{c} \mu_i \, dn_i = 0 \tag{3.1}$$

where the variations in number of moles of gaseous species i, n_i are not independent: they must conform to the element balances, which are treated as constraint equations. Let b_j be the total number of atoms of the jth element present in the system, as determined by the initial composition of the system. Let a_{ij} be the number of atoms of the jth element present in a molecule of chemical species i. The element balance can then be written as

$$b_j \equiv \sum_{i=1}^{c} (n_i a_{ij})_{IN} = \sum_{i=1}^{c} (n_i a_{ij})_{OUT} \quad (j = 1, 2, \cdots, k) \tag{3.2}$$

where the constituents are made up of k elements.

Thus, the constraint equations are given by:

$$\sum_{i=1}^{c} (n_i a_{ij})_{OUT} - b_j = 0 \tag{3.3}$$

The chemical potential of the ith species μ_i can be calculated by:

$$\mu_i = \overline{G}_i^0 + RT \ln\left(\frac{f_i}{f_i^0}\right) \tag{3.4}$$

where f_i is the fugacity of species i, R is the universal gas constant and T is the temperature. The superscript 0 refers to the standard state of a substance, thus $\overline{G}_i^0$ and f_i^0 are the standard Gibbs free energy and the standard fugacity of species i, respectively. Since fugacity can be expressed as the product of partial pressure P_i and a fugacity coefficient ϕ, Eq. (3.4) can also be presented as

$$\mu_i = \overline{G}_i^0 + RT \ln\left(\frac{\phi P_i}{P}\right) \tag{3.5}$$

A two stage processes work with reduced gas stream volume and high-energy density. For this reason the pressure is normally very low, and the gas approaches ideal behaviour. Therefore, f and P can take on the same value of 1 bar, and Eq. (3.4) can be rewritten as

$$\mu_i = \Delta\overline{G}_{f,i}^0 + RT \ln(y_i) \tag{3.6}$$

where y_i is the mole fraction of gas species i. $\Delta\overline{G}_{f,i}^0$ is the standard Gibbs free energy of formation of species i, and it is by definition zero for all the elements in their standard states. Substituting these into (3.1) and integrating gives:

$$G^{tot}(n_i, T) = \sum_{i=1}^{c} n_i \Delta\overline{G}_{f,i}^0(T) + \sum_{i=1}^{c} n_i RT \ln(y_i) \tag{3.7}$$

The problem is to find the set of n_i which minimizes the objective function G^{tot} for a specified T, subject to the constraints of the material balances (3.3).

Table 3
Chemical species considered by the equilibrium model.

Phase	Group	Chemical formula
Gas	Inorganic carbon compounds	CO, CO_2
Gas	Hydrogen/oxygen compounds	H_2, O_2, H_2O, H_2O_2, O_3
Gas	Nitrogen compounds	N_2, HCN, N_2O, NO_2, NO, NH_3
Gas	sulphur compounds	S(g), H_2S, SO_2, COS, CS_2, SO_3
Gas	Chlorine compounds	HCl, Cl_2, ClO_2
Gas	Hydrocarbons	CH_4, C_2H_4, C_2H_2, C_2H_6, C_3H_8, C_6H_6, $C_{10}H_8$, $C_{12}H_{10}$
Gas	Other organic compounds	CH_2O, CH_3OH, CH_2CO, C_6H_5OH
Gas	Other inorganic compounds	Ar
Solid	Ash compounds	SiO_2, Al_2O_3, CaO, Fe_2O_3, MgO, MnO, P_2O_5, K_2O
Solid	Carbon (char)	C(s)

3.3. Thermodynamic properties

In order to minimize the total Gibbs energy to predict chemical changes, we need to know the standard free energies of formation of each chemical species at specific temperature, $\Delta\overline{G}^0_{f,i}(T)$. For this purpose we can combine the standard enthalpy of formation, $\Delta\overline{H}^0_{f,i}(T)$, and the standard entropy of a substance, $\Delta\overline{S}^0_{f,i}(T)$, as:

$$\Delta\overline{G}^0_{f,i} = \Delta\overline{H}^0_{f,i} - T\Delta\overline{S}^0_{f,i} \tag{3.8}$$

Computational codes for equilibrium calculations require thermodynamic properties in a simple form which can be evaluated quickly, in function of temperature variations. To fill this need, polynomials approximations are often used to calculate enthalpy, heat capacity, and entropy of an ideal gas [46].

For example, the functional form for the heat capacity at constant pressure, $\overline{C}_P(T)$, is a fourth-order polynomial:

$$\frac{\overline{C}_P(T)}{R} = a_1 + a_2T + a_3T^2 + a_4T^3 + a_5T^4 \tag{3.9}$$

Values for the entropy and enthalpy can be predicted from this equation by the appropriate thermodynamic relations:

$$\frac{\overline{H}^0(T)}{RT} = \frac{b_1}{T} + \frac{\int C^0_P(T)\,dT}{RT}; \quad \frac{\overline{S}^0(T)}{R} = b_2 + \int\left(\frac{C^0_P(T)}{RT}\right)dT$$

where b_1 and b_2 are integration constants. Solving the integrals lead to a polynomials form with six constants:

$$\frac{\overline{H}^0(T)}{RT} = a_1 + a_2\frac{T}{2} + a_3\frac{T^2}{3} + a_4\frac{T^3}{4} + a_5\frac{T^4}{5} + \frac{b_1}{T} \tag{3.10}$$

$$\frac{\overline{S}^0(T)}{R} = a_1\ln T + a_2T + a_3\frac{T^2}{2} + a_4\frac{T^3}{3} + a_5\frac{T^4}{4} + b_2 \tag{3.11}$$

The standard enthalpy of formation represents the heat change associated with the formation of the substance from the elements in their most stable forms as they exist under the standard conditions of 1 atm pressure and 298 K. Thus, for all reference elements:

$$\Delta\overline{H}^0_{f,i}(298.15) = \overline{H}^0_i(298.15) = 0 \tag{3.12}$$

And for all the species

$$\Delta\overline{H}^0_f(298.15) = \overline{H}^0(298.15) \tag{3.13}$$

$$\overline{H}^0(T) = \overline{H}^0(298.15) + \{\overline{H}^0(T) - \overline{H}^0(298.15)\} \tag{3.14}$$

Note that Eq. (3.13) is equivalent to

$$\overline{H}^0(T) = \overline{H}^0_f(298.15) + \int_{298.15}^{T}\overline{C}_p(T)dT \tag{3.15}$$

The enthalpy of formation is then computed by following the definition that it is the enthalpy change associated with the formation from its stable elements at temperature T:

$$\Delta\overline{H}^0_f(T) = \overline{H}^0_{comp}(T) - \sum_{i=1}^{c}\nu_i\overline{H}^0_i(T) \tag{3.16}$$

where ν_i is the stoichiometric coefficient for element i. For example, the enthalpy of formation of CO at 1000 K is:

$$\Delta\overline{H}^0_f(1000) = \overline{H}^0(1000)CO_{(g)} - \overline{H}^0(1000)C_{(s)} - \frac{1}{2}\overline{H}^0(1000)O_{2(g)} \tag{3.17}$$

3.4. Energy balance

The computation of the basic energy balance of the two-step process is an initial and important step in the evaluation. Furthermore, the inefficiencies associated with each unit operation are incorporated in the analysis, and therefore the computation leads to a realistic estimation of the process efficiency.

Generally, in autothermal gasification, the heat generated from the exothermic reactions is consumed by the endothermic reactions, and the rest is converted to sensible heat which raises the temperature inside the reactor. The majority of the energy input to the thermal process is derived from the controlled oxidation reactions of the solid fuel at the gasifier and eventually in the converter; however, another relevant contribution in terms of energy input is that of the plasma arc for the ash vitrification. Determination of equilibrium composition at each exiting stream requires the value of the two reaction temperatures for the gasifier and the plasma converter. To obtain these values, an energy balance is performed for both steps:

$$\text{First step}\left(\sum H'\right)_{IN} = \left(\sum H'\right)_{OUT} + Q'_{loss} \tag{3.18}$$

$$\text{Second step}\left(\sum H''\right)_{IN} + W_{power} = \left(\sum H''\right)_{OUT} + Q''_{loss} \tag{3.19}$$

where

$$\left(\sum H\right)_{IN} = \sum_{r=react.} n_r\overline{H}^0_r(T_{IN}); \quad \left(\sum H\right)_{OUT} = \sum_{p=prod.} n_p\overline{H}^0_p(T_{OUT}) \tag{3.20}$$

Q_{loss} is the heat loss in the respective gasification step. We estimate this value to be 10% of the HHV of the feed stream entering the relevant conversion stage. W_{power} is the electric power supplied by the plasma arc. It comprises of the electric devices inefficiency (10%), the energy required for melting the inorganic components (10%) and the heating effect on the surrounding gas (80%). No chemical reaction was considered in the melting process.

All the enthalpies can be calculated by Eq. (3.10). For solid fuel, the definition of representative formation enthalpy based on the LHV, can be used to facilitate calculations [47]:

$$\overline{H}_{f,RDF} = \text{LHV} + \sum_{i=prod-comb} n_i\overline{H}^0_{f,i} \tag{3.21}$$

where $\overline{H}^0_{f,i}$ is the enthalpy of formation of product i under complete combustion of the RDF, and LHV is the lower heating value of the solid fuel.

3.5. The preliminary conversion process and the input data

Application of the thermodynamic equilibrium code to a two-stage process is not as straightforward as in the case of single-stage processes. One of the main requirements of a two-stage approach is that in the gasifier stage only a part of the input biomass is converted to gases while the remaining part is entrained as char into the next stage [48]. This consideration suggests that, at least in the first stage modelling, further relations that vary carbon concentration with varying process conditions should be present. The reaction network chosen for this preliminary part comprises of devolatilization of the RDF and oxidation reactions. The drying process was assumed to occur in parallel with the devolatilization. Hence, the first step of the calculation procedure is:

$$H_2O_{MOISTURE} \rightarrow H_2O_{(V)}$$

$$CH_mO_pN_qS_rCl_s \rightarrow p\text{CO} + \frac{m}{4}CH_4 + \left(1 - \frac{m}{4} - p\right)C + \frac{q}{2}N_2 + rS + \frac{s}{2}Cl_2$$

The released volatiles from pyrolysis were assumed to have been cracked into an equivalent amount of CO, CH_4, H_2O, N_2, Cl_2, sulphur and solid carbon. In this equation $CH_mO_pN_qS_rCl_s$ is the RDF brute formula, deducible from its ultimate analysis, on mois-

ture and ash free basis. Solid carbon in the form of char falls by gravity through the expanded bed, where the steam–oxygen feed ensures that it is further consumed, according to the following reactions:

$$\alpha C + O_2 \rightarrow 2(\alpha - 1)CO + (2 - \alpha)CO_2 \quad \text{where} \quad 1 \leqslant \alpha \leqslant 2$$

$$C + \beta H_2O_{Steam} \rightarrow (2 - \beta)CO + (\beta - 1)CO_2 + \beta H_2 \quad \text{where} \quad 1 \leqslant \beta \leqslant 2$$

The splitting factors α and β in the two heterogeneous reactions determine the ratio of conversion of char to carbon monoxide, carbon dioxide and hydrogen. There are empirical correlations available for the prediction of α and β. The correlations given by Linjewile and Matsui [49,50] were used in the present model giving $\alpha \approx 1.3$ and $\beta \approx 1.2$ for temperature operating in the range of 700° to 800 °C. If an excess of oxidant agents is present, they will be simply taking part in the gaseous species equilibrium, whereas if oxygen and steam are all consumed, the remaining char is treated as inert. The gasification model so conceived gives birth to a solid carbonaceous residue that, on the basis of the chemical reactions chosen for the pre-equilibrium step, if it is not further consumed, constitutes the unreacted solid carbonaceous residue from the first stage.

3.6. The solver

Various methods have been used, to date, to analyse and optimise systems and processes of this type that have been mathematically modelled as a set of non-linear equations [51]. One of the most efficient responses to the problem of analysing and optimising these types of problem is that of using the Generalized Reduced Gradient (GRG) algorithm. The calculation procedure, including the preliminary conversion process, the minimization of the objective function, as well as the mass and energy balance for the two sequential stages, can be directly solved by using a spreadsheet's Solver feature. The Solver applies the GRG method to solve the non-linear programming problem, and features an enhanced flexibility in changing the models parameters.

Fig. 4 shows the structure of the equilibrium model for the two-stage process. The first stage of gasification implies adding sufficient oxidants until all the feedstock is converted into the gaseous phase. This is covered by the first part of the model that functions independently from the iterative procedure, and is used to determine the gas composition to initiate the equilibrium calculation. When starting the iterative part, the initial value for the temperature is taken to be 500 °C, which represents the lower limit for pyrolysis to occur. This value is used for the calculation of the producer gas composition in the part of minimization of Gibbs free energy. The assumed temperature and producer gas components are then implemented into the energy balance. Solving the energy balance equations at non-equilibrium temperatures may lead to net equations. If enthalpy and heat transferred values are known for each equation, the result will be a residual net enthalpy ΔH in the energy balance, as a function of temperature:

First step

$$\left(\sum H'\right)_{IN} = \left(\sum H'\right)_{OUT} + Q'_{loss} + \Delta H' \tag{3.22}$$

Second step

$$\left(\sum H''\right)_{IN} + W_{power} = \left(\sum H''\right)_{OUT} + Q''_{loss} + \Delta H'' \tag{3.23}$$

If the value of ΔH is a negative value, the reaction temperature will be automatically reduced until becomes zero. On the other hand, if ΔH is positive, the code will automatically increase the value of temperature. After adjusting the reaction temperature, the Gibbs minimization and the energy balance routines are ran again. These iterative procedures are encompassed in a unique VBA macro-defined in the spreadsheet and are continued until the net enthalpy content from the energy balance approaches zero.

Once the procedure finds the equilibrium conditions in the first stage, the model enters the following step with those values, repeating a similar iteration for the second stage of the process. Conditions here vary essentially for the additional term in the energy balance, due to the plasma heating effect, and the secondary oxygen feed, which both increase the sensible heat contained in the product gas.

4. Experimental apparatus and materials

In order to validate the simulation results, five different solid waste (described in Table 4) gasification experimental data were used. The tests were performed in the APP demonstration plant in Swindon (UK), which is in constant use for development purpose and testing of new materials. Its major components are the following: a fluidized-bed gasifier, a biomass feeder, a plasma converter, a heat recovery unit, a dry filter, a wet scrubber and gas engines for power production.

The compact FBG employs a heated bed of calcined clay (mullite) ceramic material suspended in a rising column of hot gas. RDF feedstock is fed continuously, at a controlled rate, to the FBG through a solid fuel feeder system. In the solid fuel feeder system the as-received feed is transferred by a belt conveyor to a surge hopper where a variable-speed screw feeder modulates the volumetric feed rate of the solids at rates of up to 100 kg/h.

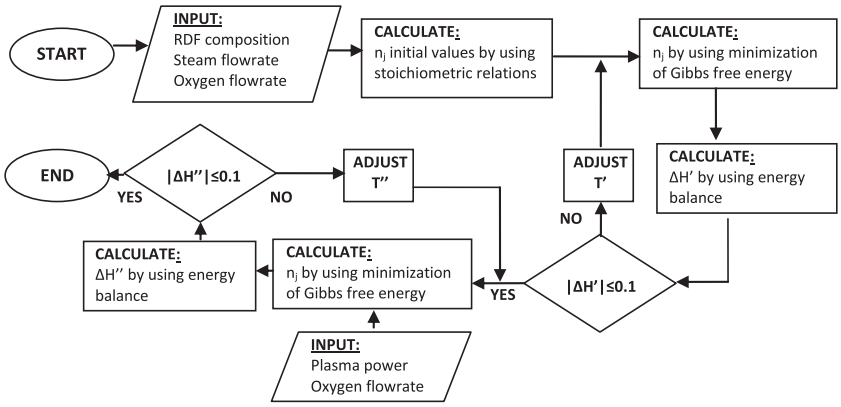

Fig. 4. Calculation procedure for a two-stage process.

Table 4
Experimental parameters and characteristics of solid wastes (as received) [52].

	Case 1	Case 2	Case 3	Case 4	Case 5
Description					
O_2/fuel ratio (w/w)	0.51	0.59	0.59	0.79	0.50
Proximate analysis, % (w/w)					
Fixed carbon	6.4	12.2	11.6	8.5	22.8
Volatile matter	59.6	50.2	64.8	47.6	68.0
Ash	19.1	23.2	12.1	8.9	0.5
Moisture	14.9	14.4	11.5	35.0	8.7
Ultimate analysis, % (w/w)					
C	41.0	47.0	43.0	31.5	45.2
H	5.7	6.3	5.6	4.1	6.46
O	17.5	6.9	26.6	19.7	45.38
N	1.2	1.74	0.61	0.4	0.26
S	0.2	0.15	0.25	0.17	0.01
Cl	0.4	0.31	0.34	0.23	0.25
GCV, (MJ/kg, dry basis)	22.1	26.4	21.0	21.0	22.0

The individual steam and oxygen feed rates are closely metered to match the feed rate of the RDF in order to ensure that the gasifier operates within the designed operating limits. The oxygen and steam feeds are mixed prior to injection through an upward facing nozzle located below the bed. Multiple pressure and temperature sensors are used to monitor and control closely the FBG operation.

In operation, the crude syngas from the gasifier flows via a refractory lined duct to the plasma converter. The desired mode of operation in the furnace is assured by changing the position of the graphite electrode. Oxygen and additional steam, if required, is axially injected into the gas stream at the point of entry into the converter. The high temperature and addition of oxidants at the converter stage promotes the cracking and reforming of organic species and gasification of sooty and char products. The power to the plasma arc is controlled to maintain the temperature of gases exiting the unit to ca. 1050–1150 °C. Ash particulates carried over from the gasifier drop out and are assimilated within the melt, which is intermittently removed from a tap hole in the bottom of the furnace.

Downstream of the plasma arc converter, the syngas is cooled from 1000 °C to 200 °C in a heat exchanger prior to treatment to remove any residual particulates and acid gas contaminants. This includes a dry filter (incorporating a ceramic filter unit with sodium bicarbonate dosing and activated carbon) followed by a wet scrubber. The refined gas is then directed to a gas engine for production of power before the oxidised gases are released to atmosphere. The demonstration plant conditions are fully automated to maintain optimal conditions at all stages of the process. Extractive sampling was used to analyse the syngas from the fluidised bed gasifier and from the plasma converter unit. The moisture content, the organic species, CO, CO_2, NOx, SOx and HCl were measured using Fourier Transform Infrared Spectroscopy (FTIR). The FTIR cannot measure diatomic molecules thus the remaining components (mainly hydrogen, nitrogen and oxygen) must be derived by difference and cross-checking calculations.

The prepared waste used from the experiments came from a number of waste treatment facilities in floc form, in a density range of 150–250 kg/m^3 and particle size between 10 and 25 mm. Table 4 presents the experimentally derived proximate analysis (wet basis), ultimate analysis (wet basis) and gross calorific value (GCV) of some of the waste usually used for trial runs. In Case 1, the RDF is prepared from blends of 50% automotive shredder residue (ASR) and 50% MSW, whereas in Case 2 it is landfill mined waste. Cases 3 and 4 treat the same RDF prepared from blend containing 50% MSW and 50% commercial and industrial (C&I) wastes, but the latter is higher in moisture content. Finally, wood pellets were tested to see the difference in the treatment of ligneous biomass (Case 5).

5. Results and discussion

5.1. Experimental validation of theoretical model data

Comparisons between experimental and theoretical model data are here reported.

Fig. 5 shows the comparison between experimental and model-predicted exit temperatures for a single stage FBG and a typical 2-stage process comprising of fluidized bed gasifier and plasma converter. The comparison is fair, with the predicted values deviating from the experimental results within the range of 3–6%; however, it is surprising that the model-predicted gasifier temperature is generally lower than the experimentally measured FBG exhaust temperature, which also tends to fluctuate significantly over time.

The reason for this will be discussed in more detail later.

Fig. 6 shows the comparison between experimental and model predicted gas compositions for a few gaseous species. As previous studies already stated [36–42], the only components present at concentrations higher than 10^{-4} mol% at equilibrium beyond 700 °C are CO, CO_2, CH_4, H_2, N_2, and H_2O. For the sake of simplicity, all the hydrocarbons measured data were enclosed in the label VOC (Volatile organic carbon). It is clearly evident that the gas stream exiting the single FBG shows a marked divergence from the predicted thermodynamic equilibrium conditions, whereas a very satisfactory agreement is found for the 2-stage process.

Two possible reasons for the discrepancy between the observed and predicted temperature and gas composition results on the first stage were investigated.

As stated in Section 3, the solid carbon, which moves to the gas phase by the Boudouard and carbon–steam endothermic reactions after the supplied oxygen is completely consumed, barely reaches an 80% conversion in reality, as also supported by numerous literature references [36,41]. Because the stoichiometry of the preliminary conversion process is usually beyond the carbon boundary point, which is obtained when exactly enough gasifying medium is added to avoid carbon formation and achieve complete gasification, its direct application to the gasifier stage implicitly considers a 100% complete carbon conversion. That results in some discrepancy in predicting gas composition and temperature in the gasifier. Furthermore, an examination of the gasifier exit gas composition (Fig. 6) revealed that up to 10% methane and other volatile organics were present in the measured data, while almost no methane formation was predicted by the model. VOC formation has a double effect on the exhaust temperature. First, its formation is exothermic, and second, for a given biomass carbon conversion, production of methane and other short-chain hydrocarbons decreases the production of CO and H_2, both of which are endothermic in nature. This also explains why the measured concentration of CO and H_2 is much lower than would be predicted from theory.

It is worthwhile to note that the experimental results obtained from the single and 2-stage treatment of several feedstock types are in line with each other. Only for the treatment of wood pellets (Case 5) they are notably different, especially in the FBG unit. Fig. 6 shows that in this case the levels of organics out of the first stage are lower, whereas the concentrations of CO and H_2 are more closely in line with thermodynamic predicted values. The reason can be imputed to one of the most notable differences between RDF (especially those which are high in plastics like in Case 3) and ligneous biomass. The latter is lower in ash content and has a higher level of "fuel oxygen" which would be immediately available to take part in the gasification reactions during the preliminary thermal decomposition (pyrolysis) occurring in the first stage. This

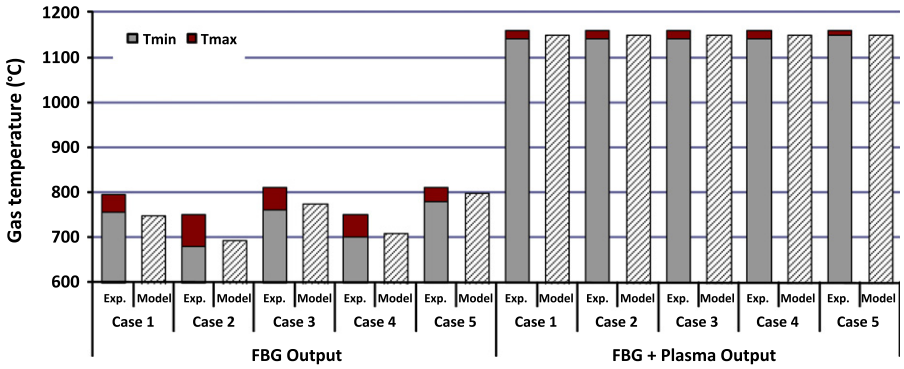

Fig. 5. Comparison of experimental temperature ranges with equilibrium temperatures used in the model in the: (left) FBG gasifier; (right) FBG + Plasma converter.

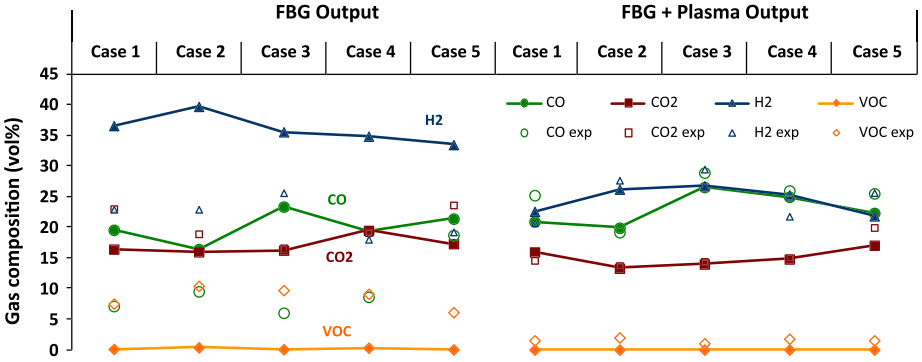

Fig. 6. Comparison of gas composition predicted by the model with experiment data from (left) FBG gasifier; (right) FBG + Plasma converter. Note: out of the second stage the fraction of the single component over the total volume is lowered by the presence of plasma gas (Argon).

characteristic overcomes in part the issues related with transport phenomena and flow mixing between the particles and the gaseous species within the first stage, promoting the carbon conversion and enhancing the kinetics of gasification reactions. These differences in the syngas quality are in effect reduced in the second stage, due to the flexibility of the system in "tuning" the power demand with the oxygen partition, optimizing the conversion of char from different waste types.

The compositions of the predicted and the actual syngas out of the entire process are virtually identical and include also the inert gas (mainly Argon) used for general inerting duties. Note that these values are for a gas generated in the demonstration plant unit which contains relatively higher levels of inert gases than would occur in an industrial system. When the effect of the plasma gas is accounted for, the hydrogen concentration is around 30% in volume, and the projected GCV of the syngas is usually around 10 MJ/kg.

The actual conversion is also influenced to some extent by the effective CO/CO_2 ratio, with higher ratios leading to marginally higher conversions, hence approaching the thermodynamic equilibrium conditions. In the 2-stage process a complete conversion is achieved, and this is more evident from the comparison of process parameters in Fig. 7, where CO/CO_2 and H_2/CO mole ratio data from experimental trial runs processing different wastes are normalised for direct comparison. On the plasma side, the comparison is good, showing that the carbon conversion efficiency and syngas quality achieved using a high-temperature 2-stage process tends to be higher than many other systems operating in a single stage. This is in part due to the further conversion of residual tars and chars into volatile carbon components such as carbon monoxide and methane. in the plasma converter. Furthermore, the high capture efficiency of fly ash along with the vitrification converter system, allows the residual carbon in the ash to react with the gas-phase to form more CO and CO_2.

5.2. Energy efficiency

Once it is established that for a thermal two-stage gasification process the product composition can be predicted from thermodynamics, one can proceed to impose process specific arrangements to optimize the performance of the process. The first step of the process is a preliminary conversion of RDF which produces mainly pyrolysis gas, ash, and char, along with other liquid organic contaminants. As for now, char is not used in the process. Hence, conditions should be chosen to maximize the energy content of the raw syngas. Two major process specific limitations are identified at the first stage: a lower limit temperature for the kinetics of gasification reactions, and an upper limit temperature at which ash sintering and agglomeration become important issues. Reported experimental data on RDF gasification in fluidized bed reactors indicate that these temperatures are about 680 and 820 °C, respectively [22]. These values then set the limits on the amount of oxygen required at this stage. As already said in Section 2, a single stage unit would also depend stoichiometrically on the oxygen supply to sustain the partial oxidation reaction of char, with a minimum oxygen–carbon ratio of about 0.4–0.5 required. However, in a two-stage process there is no limit on the overall oxygen to carbon ratio, for the char conversion is completed in the second stage by the aid of the plasma arc power.

The second step of the process is the complete char conversion and thermal tar cracking which breaks the pyrolysis gas down to a syngas mixture containing only CO, CO_2, H_2, and H_2O. There are not particular temperature limitations in the plasma converter; however, the process conditions should be chosen to minimize the

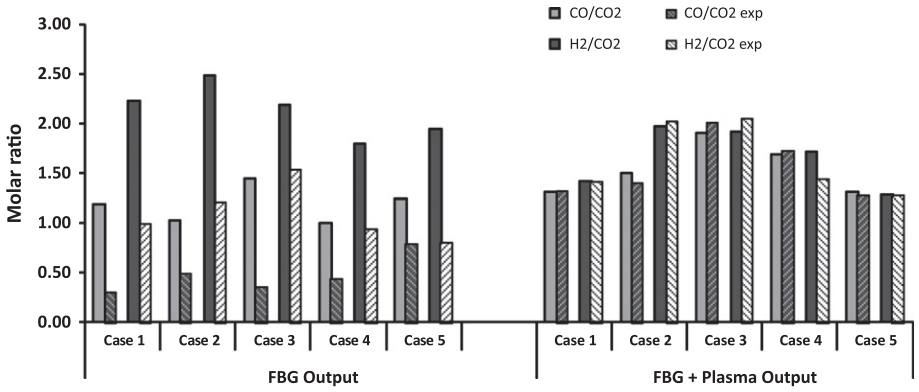

Fig. 7. Comparison of model results with experiment data from the (left) FBG gasifier; (right) FBG + Plasma converter.

amount of power supplied by the plasma electrode. Tars, aromatic compounds and the remaining char can undergo partial oxidation by precisely controlling the amount of the secondary oxygen inlet fed into the plasma-arc reactor. The heat released in the exothermic reactions provides additional thermal energy for the primary gasification reaction to proceed very rapidly, reducing the heating power required by the plasma electrode.

As the composition of the syngas is one of the variables to be considered, the process optimization has to be performed for both steps simultaneously. The parameters which can be varied are the steam to O_2 ratio in the FBG unit and the plasma arc electrical power demand in relation with the secondary oxygen inlet in the plasma converter.

Fig. 8 shows the effect of steam to oxygen ratio on the final syngas quality. As the steam/oxygen ratio increases the CO/CO_2 ratio decreases, while the H_2/CO ratio increases.

Such shifts in gas composition with increasing steam/oxygen ratio are strongly indicative of increasingly favourable conditions for hydrogen formation in accordance with the water gas shift reaction. However, steam addition reduces the temperature of gasification and more oxygen has to be added to maintain the temperature level, lowering the heating value of the fuel gas produced. In a two-step process this does not necessarily represent an issue; as we discussed before, a two-step thermal process can work with lower oxygen to carbon ratio compared to conventional single-stage gasification.

In order to evaluate whether the steam addition in the FBG positively compensates for the plasma power demand in the second stage, the relationship among plasma power and heating value variation should be considered synthetically. The cold gas efficiency (CGE) is a standard criterion that is frequently quoted for traditional gasification process. This concept is modified and applied to a two-stage gasification process in this model:

$$CGE = \frac{\dot{m}_{syngas}\mathrm{GHV}_{syngas}}{\dot{m}_{RDF}\mathrm{GHV}_{RDF} + W_{power}} \tag{5.1}$$

where $\dot{m}_{\mathrm{syngas}}$ and $\dot{m}_{\mathrm{RDF}}$ denote the mass flow rates of syngas and feedstock, while $\mathrm{GHV}_{\mathrm{syngas}}$ and $\mathrm{GHV}_{\mathrm{RDF}}$ mean the gross heating values of syngas and feedstock on mass basis. W_{power} denotes the power of plasma supplied in the arc electrode. By keeping constant the oxygen inlet at the first stage, Fig. 9 shows how the ratio between the oxygen injected in stage-two and the total injected oxygen (oxygen partition ratio or OPR) affects the cold gas efficiency of the process.

An increase in secondary oxygen inlet flowrate is generally accompanied by reduced plasma power consumption, thus maintaining a constant high level of thermal energy to complete the gas reforming. In fact, keeping constant the temperature of the

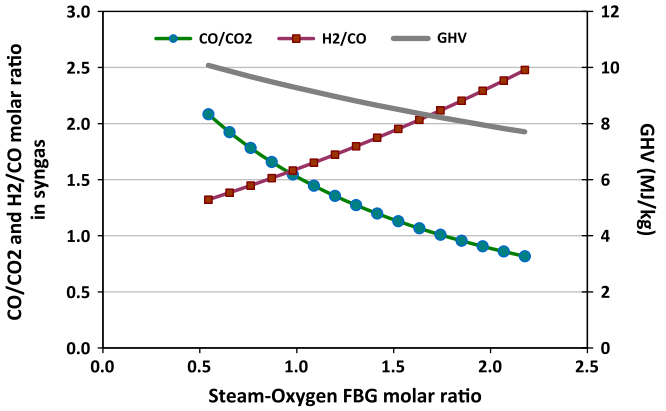

Fig. 8. Effect of steam/oxygen ratio in the FBG stage on outlet syngas quality (Case 1).

syngas exiting the plasma converter, the increase in this parameter involves a greater extent of the exothermic reactions, and, as a consequence, a lower electric power W_{power} is required by the plasma arch torch.

With the increase of secondary oxygen intake (i.e. higher OPR), the change of CGE can be divided into two different parts. Initially, when OPR increases from 0 (i.e. no secondary oxygen inlet) to near 0.2, the CGE decreases slowly and approximately linearly from 0.83 to 0.80 (Case 2). This irrelevant change may be explained by a self-compensating effect determined by a lower GHV with decreasing the power consumption. If on the one hand, an increase in W_{power} should in fact lower the CGE, on the other hand plasma action plays a crucial role in the process of conversion of char to CO rather than CO_2, enhancing significantly the gas heating value, which is key in Eq. (5.1).

On this evidence, when reducing to zero the plasma input, whilst greatly enhancing the oxygen, the syngas quality is significantly diminished, leading to a more rapid decrease in CGE. The additional oxygen supplies the required heat by reacting with the reactive syngas, and hence, the ultimate CGE is drastically reduced by virtue of the low GHV having a predominant role; that is, by the time the system reaches the high temperature required for ash vitrification and tar reforming, more gas reacted to form H_2O and CO_2. Similar trends for syngas GHV and CGE are found for different feedstock cases.

Fig. 9 shows the enormous benefit of working in combination with plasma and fuel oxidant streams. It is clear that the energy efficiency for the process sharply decreases when plasma is switched off. Thus, it would not be profitable to alter the gasification extent only by increasing the oxidant inlet.

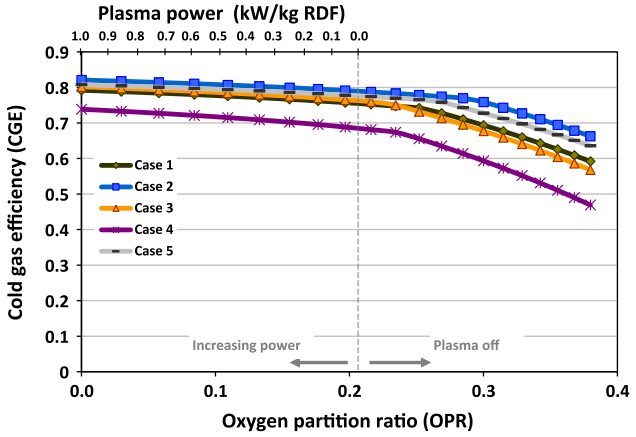

Fig. 9. Effect of oxygen partition ratio and plasma arc power on overall process performance.

Different applications suggest the operational ranges where the second stage conversion takes place.

Depending on the RDF's calorific value and ash/moisture content, the operational range of this second stage is determined by fixing one or more quality parameters, e.g. the final GHV. A typical case is the syngas generated limiting the plasma power between 0.15 and 0.2 kW/kg RDF. This clean syngas has a GHV in the range of 9–13 MJ/kg, and is widely suitable for electric power generation via gas engine in the range of 0.95–1.27 MWh/t RDF with a net electrical efficiency (NEE) of 23–30% [12].

However, the choice of the parameter values does not only depend on the thermal value of the syngas or on the thermodynamic efficiency of the process but also on the potential use for the cleaned gas generated. Let us consider, for example, the use as precursor for synthesis of natural gas (BioSNG), which is a typical case. A high H_2/CO ratio is required, and the use of only plasma, with eventually additional steam, may be essential for the process. Hence the optimum choice of operation parameters should be based on the detailed process requirements for different projects.

6. Conclusion

Despite the unfavourable characteristics of RDF and the complex design of the system, the sequential gasification + reforming equilibrium modelling considered in this study can reach good process parameters predictions and appealing energy performance testing capabilities. The study effectively demonstrated that the two-stage gasification system significantly reduces the concentration of condensable tars in the syngas, improving the gas yield of the system and the carbon conversion efficiency which is crucial in other single stage systems. There is close correlation between the observed and predicted values of the syngas exiting the plasma converter, although the actual level of CO is still ~1% below the theoretical value while the CO_2 level is 1.5% higher. The noted differences are likely due to flow and RDF composition uncertainties rather than from the predictive model. Given the size and configuration of the demonstration plant and the inherent variability of real RDF uncertainties are to be expected.

On the contrary, the known deficiencies of single stage process, have led to the theoretical prediction of the gas composition at the exit of the first stage deviating significantly from the values derived from the trials. It is evident that there are rate controlling mechanisms operating, including the rate of cracking of the organics and the rate of mass transport of the bulk oxidants to the surface of the fuel which make the equilibrium model unsuitable for the FBG, and in general for any single stage process operating with solid wastes. From a practical point of view, this is of no consequence, as the gasification reactions are completed in the plasma converter and it is the composition of the gas output from the second stage which is critical. The equilibrium condition is always attained for high temperatures and long residence time; thus, the model proposed in this work is suitable for predicting in a two-stage thermal conversion technology. The layout of syngas LHV and CGE have been calculated and analyzed. It was found out that high GHV and CGE values are maintained in different power and oxygen conditions. The reason is that addition of plasma power into the converter decreases the amount of secondary oxygen required for complete gasification and produces larger amounts of CO and H_2 in the product gas. The optimizing direction for the two-stage process can only be determined after considering the detailed aim and situation on different projects.

Acknowledgements

The Authors acknowledge financial support for this project from University College London (UCL) via an Impact Studentship co-funded by APP.

References

[1] Fichtner Consulting Engineers. The viability of advanced thermal treatment of MSW in the UK. ETSET report; 2004.
[2] Siedlecki M, de Jong W. Biomass gasification as the first hot step in clean syngas production process – gas quality optimization and primary tar reduction measures in a 100 kW thermal input steam–oxygen blown CFB gasifier. Biomass Bioenergy 2011;35(Suppl. 1):S40–62.
[3] Meng X, de Jong W, Fu N, Verkooijen AHM. Biomass gasification in a 100 kWth steam–oxygen blown circulating fluidized bed gasifier: effects of operational conditions on product gas distribution and tar formation. Biomass Bioenergy 2011;35(7):2910–24.
[4] Na JI, Park SJ, Kim YK, Lee JG, Kim JH. Characteristics of oxygen-blown gasification for combustible waste in a fixed-bed gasifier. Appl Energy 2003;75(3–4):275–85.
[5] Basu P, Kaushal P. Modeling of pyrolysis and gasification of biomass in fluidized beds: a review. Chem Prod Process Model 2009;4(1).
[6] Rao MS, Singh SP, Sodha MS, Dubey AK, Shyam M. Stoichiometric, mass, energy and exergy balance analysis of countercurrent fixed-bed gasification of post-consumer residues. Biomass Bioenergy 2004;27(2):155–71.
[7] Kim S, Park H, Kim. H. 100 kW steam plasma process for treatment of PCBs (polychlorinated biphenyls) waste. Vacuum 2003;70(1):59–66.
[8] Nema SK, Ganeshprasad KS. Plasma pyrolysis of medical waste. Curr Sci 2002;83(3):271–8.
[9] Cheng TW, Ueng TH, Chen YS, Chiu JP. Production of glass-ceramic from incinerator fly ash. Ceram Int 2002;28(7):779–83.
[10] Ducharme C, Themelis N. Analysis of thermal plasma-assisted waste to energy processes. In: Proceedings of the 18th annual North American waste to energy conference NAWTEC18; 2010.
[11] Helsen L, Bosmans A. Waste-to-energy through thermochemical processes matching waste with process. In: First international symposium on enhanced landfill mining, Belgium: Houthalen-Helchteren; 2010.
[12] APP. Internal document, unpublished. Pre-enquiry document – 100719; July 2004.
[13] Ghani WAWAK, Alias AB, Cliffe KR. Co-combustion of refuse derived fuel with coal in a fluidised bed combustor. J Eng Sci Technol 2009;4(1):122–31.
[14] Gomez-Barea A, Nilsson S, Barrero FV, Campoy M. Devolatilization of wood and wastes in fluidized bed. Fuel Process Technol 2010;91(11):1624–33.
[15] Albal RS, Litka AF, Neoh KG, Westra LF, Woodroffe JA, Stickler DB, et al. Advanced two-stage gasification system. 1. Experimental results. Ind Eng Chem Res Â® 1989;28(11):1600–7.
[16] Hamel S, Hasselbach H, Weil S, Krumm W. Autothermal two-stage gasification of low-density waste-derived fuels. Energy 2007;32(2):95–107.
[17] Chopra S, Jain A. A review of fixed bed gasification systems for biomass. Agric Eng Int: CIGR Ej Invited Overview 2007;IX(5).
[18] Yang Z et al. Dynamic model for an oxygen-staged slagging entrained flow gasifier. Energy Fuels 2011;25:3646–56.
[19] Ciferno J, Marano J. Benchmarking biomass gasification technologies for fuels, chemicals and hydrogen production. US Department of Energy, National Energy Technology Laboratory. Published June 2002. National Energy Technology Laboratory (NETL). <http://www.netl.doe.gov/technologies/coalpower/gasification/pubs/market.html> [accessed 1.04.10].
[20] Kersten SRA, Wang X, Prins W, Van Swaaij WPM. Biomass pyrolysis in a fluidized bed reactor. Part 1: Literature review and model simulations. Ind Eng Chem Res 2005;44(23):8773–85.

[21] Hallgren A. Improved technologies for the gasi cation of energy crops. Publishable final report (TPS AB), European Commission JOULE III Programme, Project No. JOR3-CT97-0125.
[22] Devi L, Ptasinski J, Janssen FJJG. A review of the primary measures for tar elimination in biomass gasification processes. Biomass Bioenergy 2003;24:125–40.
[23] Campoy M, Gómez-Barea A, Fuentes-Cano D, Ollero P. Tar reduction by primary measures in an autothermal air-blown fluidized bed biomass gasifier. Ind Eng Chem Res 2010;49(22):11294–301.
[24] Gallagher MJ, Fridman A. Plasma reforming for H_2-rich synthesis gas. Fuel Cells: Technol Fuel Process 2011:223–59 [chapter 8].
[25] Fridman A, Gutsol A, Gangoli S, Ju Y, Ombrello T. Characteristics of gliding arc and its application in combustion enhancement. J Propul Power 2008;24(6):1216–28.
[26] Lemmens B, Elslander H, Vanderreydt I, Peys K, Diels L, Oosterlinck M, et al. Assessment of plasma gasification of high caloric waste streams. Waste Manage 2007;27(11):1562–9.
[27] Fridman A, Kennedy LA. Plasma physics and engineering. New York: Taylor and Francis; 2004.
[28] Gomez E, Rani DA, Cheeseman CR, Deegan D, Wise M, Boccaccini AR. Thermal plasma technology for the treatment of wastes: a critical review. J Hazard Mater 2009;161(2–3):614–26.
[29] Morrin S, Lettieri P, Chapman C, Mazzei L. Two stage fluid bed-plasma gasification process for solid waste valorization: technical review and preliminary thermodynamic modelling of sulphur emissions. Waste Manage 2012;32(4):676–84.
[30] Whitty KJ, Zhang HR, Eddings EG. Emissions from syngas combustion. Combust Sci Technol 2008;180(6):1117–36.
[31] Scur P, Rott A. Environmental compatibility and plant safety when using secondary materials at the rüdersdorf cement works. ZKG Int 1999;52(11): 596–607.
[32] Arena U. Process and technological aspects of municipal solid waste gasification. A review. Waste Manage 2012;32:625–39.
[33] EUROPLASMA. Production d'électricité par gazéification – Energies renouvelables et développement durable. Project CHO-Power – Morcenx, <http://www.paris-dechets.com/medias/interventions /a10/ a10_marc_lefour_production_electricite_gazeification.pdf>; 2008. [retrieved 21.12.09]
[34] EBARA. EUP – EBARA UBE Process for gasification of waste plastics. <http:// www.ebara.ch/>; 2003. [retrieved 05.2010]
[35] Fujimura H, Oshita T, Naruse K. Fluidized bed gasification and slagging combustion system. In: Presented at the IT3 conference, <http:// www.ebara.ch/>, Philadelphia (USA); 2001. [retrieved 05.12]
[36] Petersen I, Werther J. Three-dimensional modeling of a circulating fluidized bed gasifier for sewage sludge. Chem Eng Sci 2005;60(16):4469–84.
[37] Jarungthammachote S, Dutta A. Thermodynamic equilibrium model and second law analysis of a downdraft waste gasifier. Energy 2007;32(9): 1660–9.
[38] Li XT, Grace JR, Lim CJ, Watkinson AP, Chen HP, Kim JR. Biomass gasification in a circulating fluidized bed. Biomass Bioenergy 2004;26(2):171–93.
[39] Jarungthammachote S, Dutta A. Equilibrium modeling of gasification: Gibbs free energy minimization approach and its application to spouted bed and spout-fluid bed gasifiers. Energy Convers Manage 2008;49(6):1345–56.
[40] Barba D, Prisciandaro M, Salladini A, Mazziotti Di Celso G. The gibbs free energy gradient method for RDF gasification modelling. Fuel 2011;90(4):1402–7.
[41] Jand N, Brandani V, Foscolo PU. Thermodynamic limits and actual product yields and compositions in biomass gasification processes. Indus Eng Chem Res 2006;45(2):834–43.
[42] Melgar A, Pérez JF, Laget H, Horillo A. Thermochemical equilibrium modelling of a gasifying process. Energy Convers Manage 2007;48(1):59–67.
[43] Prins MJ, Ptasinski KJ, Janssen FJJG. From coal to biomass gasification: comparison of thermodynamic efficiency. Energy 2007;32(7):1248–59.
[44] Bruni G, Solimene R, Marzocchella A, Salatino P, Yates JG, Lettieri P, et al. Self-segregation of high-volatile fuel particles during devolatilization in a fluidized bed reactor. Powder Technol 2002;128(1):11–21.
[45] Gómez-Barea A, Leckner B. Modeling of biomass gasification in fluidized bed. Progr Energy Combust Sci 2010;36(4):444–509.
[46] Mc Bride BJ, Gordon S, Reno MA. Coefficients for calculating thermodynamic and transport properties of individual species. NASA Technical Memorandum 4513; 1993.
[47] De Souza-Santos LM. Solid fuels combustion and gasification: modeling, simulation, and equipment operations. 2nd ed. New York: Taylor and Francis; 2010.
[48] Abichandani JS, Woodroffe JA. Advanced two-stage gasification system. 2. Process evaluation. Indus Eng Chem Res® 1989;28(11):1607–13.
[49] Linjewile TM, Agarwal PK. The product CO CO_2 ratio from petroleum coke spheres in fluidized bed combustion. Fuel 1995;74(1):5–11.
[50] Matsui I, Kunii D, Furusawa T. Study of fluidized bed steam gasification of char by thermogravimetrically obtained kinetics. J Chem Eng Jpn 1985;18(2): 105–13.
[51] Edgar TF, Himmelblau DM. Optimization Of chemical processes. 2 Rev ed. Mcgraw-Hill Publishing Co.; 2001.
[52] Ray R, Taylor R, Chapman C. The deployment of an advanced gasification technology in the treatment of household and other waste streams. Process Saf Environ Prot 2012;90(3):213–20.